Antibacterial and pH-Responsive Chitosan/Glutaraldehyde Film with Red Cabbage Anthocyanins for Meat Freshness Detection

Faza Ilya Sururim Masfufah[1], Ngadiwiyana Ngadiwiyana[1], Yassaroh Yassaroh[2], Retno Wulandari[3] and Nor Basid Adiwibawa Prasetya[1,*]

[1]Department of Chemistry, Faculty of Science and Mathematics, Universitas Diponegoro, Jl. Prof. H. Soedarto SH, Tembalang, Semarang, 50725, Indonesia

[2]Research Center for Mining Technology - National Research and Innovation Agency (BRIN), KS Iskandar Zulkarnain, Ir. Sutami street km. 15, Tanjung Bintang, Lampung Selatan 35361, Indonesia

[3]Research Center for Polymer Technology, National Research and Innovation Agency (BRIN), KST BJ. Habibie, Puspiptek Area Building 460, Tangerang Selatan 15314, Indonesia

(*Corresponding author's e-mail: nor.basid.prasetya@live.undip.ac.id)

Abstract

This study presents the development of a biodegradable chitosan-based film responsive to pH changes, utilizing anthocyanins from red cabbage extract as a natural pH indicator. Chitosan films were prepared with varying volumes of glutaraldehyde (GA) as a cross-linking agent through a casting method, followed by coating with red cabbage extract. The chitosan/GA films exhibited color transitions within a pH range of 2 - 13, changing from purple during the initial storage to green as chicken meat spoiled, effectively indicating freshness. FE-SEM analysis revealed that GA cross-linking resulted in a denser film structure, with a reducing porosity from 10.0% (pure chitosan) to 6.7% (chitosan/GA). The incorporation of glutaraldehyde significantly enhanced the films' tensile strength, with the optimal strength achieved at 0.5 mL GA, representing a threefold increase compared to pure chitosan. The films also demonstrated improved mechanical stability, defined as an improved resistance to deformation under applied stress, which is crucial for packaging integrity. Additionally, glutaraldehyde modified films exhibited greater hydrophilicity, as indicated by changes in contact angle, and displayed antibacterial activity, with CG0.5 exhibiting the largest inhibition zone against *S. aureus* (4.9 mm). Although GA incorporation slightly reduced the biodegradation rate, the films still displayed acceptable biodegradability, defined as the ability to degrade by least 60% within 5 days sufficient for short-term food packaging applications. The red cabbage extract-coated chitosan-GA films effectively monitored meat spoilage through visible color changes and demonstrated eco-friendly degradation behavior, positioning them as promising smart packaging materials for chicken meat freshness monitoring.

Keywords: pH sensitive, Glutaraldehyde, Biodegradability, Chicken freshness, Smart packaging film, Antibacterial activity

Introduction

Food packaging is important from the consumer's perspective in modern commercial trade, as it directly impacts the freshness and quality of food products [1,2]. This necessity has driven the development of innovative packaging systems that provide consumers with quick, easy-to-understand, and accessible information about the quality of the purchased food [3]. Smart packaging systems refer to advanced packaging systems that enable real-time monitoring of food quality [4]. These systems typically incorporate biopolymer matrices combined with pH indicators to monitor changes in food conditions.

The development of packaging materials based on natural polymers has been a prominent research focus, primarily due to the biodegradable nature of these materials, which helps mitigate environmental waste accumulation. Among these natural polymers, chitosan (1-4 linked 2-amino-deoxy-β-D-glucan) stands out due to its widespread availability, ease of extraction, high transparency, antibacterial properties, and biodegradability. These characteristics make chitosan a promising candidate for bioplastics production [5-7].

Regarding pH indicators, natural materials that contain anthocyanins are frequently utilized in smart packaging systems, with anthocyanin being among the most preferred choices. Anthocyanins are secondary metabolites found in various fruits and vegetables, such as red cabbage, sweet potatoes, grape skins, and peanut skins. These compounds exhibit a broad of colors that shift in response to pH levels. Making them highly attractive and environmentally friendly pH indicators [8]. The color transition of anthocyanins is attributed to the presence of phenolic or conjugated groups within their structure, which undergo structural transformations in response to pH change. Additionally, external factors such as temperature and copigmentation can further influence these color variations [9,10].

On the primary applications of pH indicators in smart packaging is food freshness monitoring. Food spoilage, particularly in perishable items such as fish, meat, and shrimp, is often associated with the release of volatile compounds, including amine gases. These gases alter the surrounding acid-base balance, ultimately to pH changes [11,12]. This, tracking food spoilage through pH variations presents an effective and practical approach. A visual detection system based on pH changes offers significant advantages for customers, as it enables them to assess food freshness directly through observable color shifts in the packaging [13]. Consequently, anthocyanins play a crucial role as natural pH indicators, integrating seamlessly into smart packaging systems to enhance food safety and quality.

In recent years, several studies have explored the use of biopolymers and anthocyanins as pH indicators, particularly for application in food freshness monitoring. Previous research has developed pH-responsive smart films based on gelatin-based film incorporated red cabbage extract as a natural color indicator [14]. Additionally, chitosan/methylcellulose films containing anthocyanin from *Phyllanthus reticulatus* have been successfully employed to monitor the freshness of fish fillets [15].

One approach to enhancing the performance of biopolymer films is the incorporating of glutaraldehyde (GA), which serves as a cross-linking agent to improve the mechanical properties of chitosan-based films [4,16]. These improvements are essential for smart packaging applications, where mechanical robustness and structural stability are critical [17]. In addition, glutaraldehyde is also able to improve the antibacterial properties of chitosan Hasanvand *et al.* [18], Li *et al.* [19], which supports better packaging materials. These enhanced properties make chitosan a more effective barrier against microbial contamination, ultimately extending the shelf life of products. As a result, the combination of glutaraldehyde and chitosan presents a promising solution for the development of safer and more durable packaging options.

Although previous studies have explored chitosan-based pH-responsive films, the development of GA-cross-liked chitosan films with pH sensitivity remain largely unexplored. Therefore, this study aimed to develop smart chitosan-based films cross-linked with GA and infused with red cabbage (*Bassica oleracea*) extract as visual sensors for monitoring the freshness of chicken meat. The developed films were systematically evaluated in terms of their chemical structure, mechanical properties, and effectiveness as freshness indicators through observable color changes. This research offers novel insight into the development of biopolymers-based smart films for food freshness monitoring, while providing an environmentally friendly alternative to synthetic sensors.

Materials and methods

Materials

Chitosan powder (molecular weight of 75.02 KDa, degree of deacetylation 98.03%) was used as the primary materials, glutaraldehyde (*Merck*, for synthesis) served as the crosslinking agent, and fresh red cabbage (obtained from Tangerang, Indonesia) was used as the raw material for extracting the natural pH indicator (anthocyanin). Hydrochloric acid (HCl, 37%, *Merck*, for analysis), acetic acid (CH$_3$COOH, *Merck*, for analysis), sodium hydroxide (NaOH, *Merck*, for analysis), ethanol (C$_2$H$_5$OH, *Smart-Lab*, analytical reagent), and distilled

water (aquadest, H_2O) were used as solvents and reagents in the film preparation and analysis processes.

Preparation of pH-indicative chitosan film
Extraction of anthocyanins from red cabbage

The red cabbage extract was prepared following the procedure outlined by Araujo *et al.* [20], with slight modifications. The red cabbage was chopped into small pieces and dried in a vacuum oven at 40 °C and 0.08 Pa for 7 h before being exposed to the solvent. After drying, the cabbage was macerated at a 1:4 (w/v) ratio using 25% ethanol at pH 4.01, with hydrochloric acid used to adjust the pH. The solution was stored in a dark environment at 5 °C for 24 h. It was then filtered using Whatman filter paper No. 4, and the resulting extract

was concentrated using a vacuum rotary evaporator until the solvent was fully evaporated.

Preparation of pH-indicative chitosan film

To prepare a 2% chitosan solution (**Table 1**), 0.3 g of chitosan was dissolved in 15 mL of 1% acetic acid with continuous stirring at room temperature. After ensuring complete dissolution, varying volumes of 1% glutaraldehyde (GA) were added to the solution as a cross-linking agent. The solution was poured into a silicone mold (8×6 cm²) and dried in an oven at 37 °C for 24 h to evaporate the solvent, producing the final purple smart film. After dried, 1.1 mL of red cabbage anthocyanin extract was coated into the film.

Table 1 Chitosan/GA films composition.

Sample	Chitosan (g)	GA 1% (mL)	Red cabbage extract (mL)
CG0.0		0.0	
CG0.5	0.3	0.5	1.1
CG1.0		1.0	
CG1.5		1.5	

Red cabbage extract testing
Anthocyanin content of red cabbage extract

A pH solution of 1.0 and 4.5 was prepared using HCl and NaOH. The extract was then dissolved in the pH solution at a 1:4 (v/v) ratio, and the absorbance of each solution was measured using a UV-Vis spectrophotometer (UH5300, Indotech Scientific) at wavelengths of 520 nm and 700 nm. The obtained absorbance values were used to calculate the anthocyanin content using formulas (1) and (2) [21]:

$$A = (A520 - A700)pH1.0 - (A520 - A700)pH4.5 \quad (1)$$

$$\text{Total anthocyanin (mg/L)} = \frac{A \times MW \times DF \times 1000}{(E \times W)} \quad (2)$$

Where A is the absorbance, MW is molecular weight (g/mol), E is the molar absorption coefficient (26,900 $L.mol^{-1}.cm^{-1}$, expressed as cyanidin-3-glucoside), W is the path length of the cuvette (1 cm), and DF is the dilution factor.

pH response of red cabbage extract

The color response of the red cabbage extract and the films was evaluated across a pH range of 2 - 13. The pH of distilled water was adjusted using HCl and NaOH. A 30 µL sample of red cabbage extract and film pieces (1×1 cm²) were placed in separate wells of a drip plate. Both the extract and the film were immersed in the prepared pH solutions, and the resulting color changes were documented using a camera.

Characterization and testing of chitosan/GA-red cabbage films
Characterization of chitosan/GA-Red cabbage films

The obtained films were analyzed for their functional groups using FTIR in ATR mode. The films were cut into 1×1 cm² pieces, and their FT-IR spectra were recorded using a Brucker Alpha II spectrometer with a resolution of 4 cm^{-1}, operating within the 400 - 4000 cm^{-1} range. The surface morphology and cross-sectional structure of the films were examined using FE-SEM (JSM IT700HR). The tensile properties of the

films were evaluated with a Universal Testing Machine Shimadzu (type AG-X Plus 50 kN) in accordance

ASTM D882, at a crosshead speed of 5 mm/min). Five rectangular specimens (6×1 cm²) from each film type were tested. The films were clamped between the machine grips, and tensile tests were conducted to determine Young's modulus, tensile strength, and elongation at break from the resulting stress–strain curves. Additionally, sessile drop contact angle analysis was performed using a Kruss drop shape analyzer. The contact angle, which reflects the surface's hydrophilicity or hydrophobicity, was measured by placing a distilled water droplet on the film.

Antibacterial activity testing of the film

The antibacterial activity of the chitosan film against the pathogenic bacteria *S. aureus* (G$^+$) was evaluated using the disk diffusion method. A fresh bacterial culture (100 µL, 10^8 CFU/mL) was spread on Mueller Hinton Agar's (MHA) surface, and circular film samples (6 mm diameter) were placed in petri dishes. After incubator for 24 h at 35°C in a thermostatic incubator (Sanyo Gallenkamp MIR-252/LD. 0560), the inhibition zone surrounding the films were measured with a ruler and recorded in millimeters.

Film soil degradability

Small pieces of the dry films (2×1 cm²) were weighed and buried in the soil. The percentage of weight loss was measured daily over 5 days to evaluate the films' biodegradability.

Film transparency

The chitosan film was placed on a white sheet of paper before and after coating with red cabbage extract. The transparency of the films was observed and documented by photographing them using a camera.

Application for monitoring of chicken freshness

Fresh chicken meat was purchased from a local traditional market in Semarang, Indonesia, and transported to the laboratory. Meat samples (10 g) were placed in sterile petri dishes, and each film (2×2 cm²) was attached to the surface of the meat. The plates were incubated at room temperature for 1 to 3 days, during which time any color changes on the films were documented using a camera.

Results and discussion
Red cabbage extract testing

Red cabbage extract was successfully extracted, producing a thick purple solution. The anthocyanin content of the extract using a 25% ethanol solvent at pH 4 was found to be 193 mg/L. This result aligns with the findings of Araujo *et al.* [20], who reported that 25% ethanol and pH 4 provide optimal conditions for extracting and preserving anthocyanins in red cabbage, resulting in maximum anthocyanin yields. Extraction solvents with lower pH values tend to produce higher anthocyanin concentrations, as phenolic compounds exhibit a greater affinity to acidic environments [22,23].
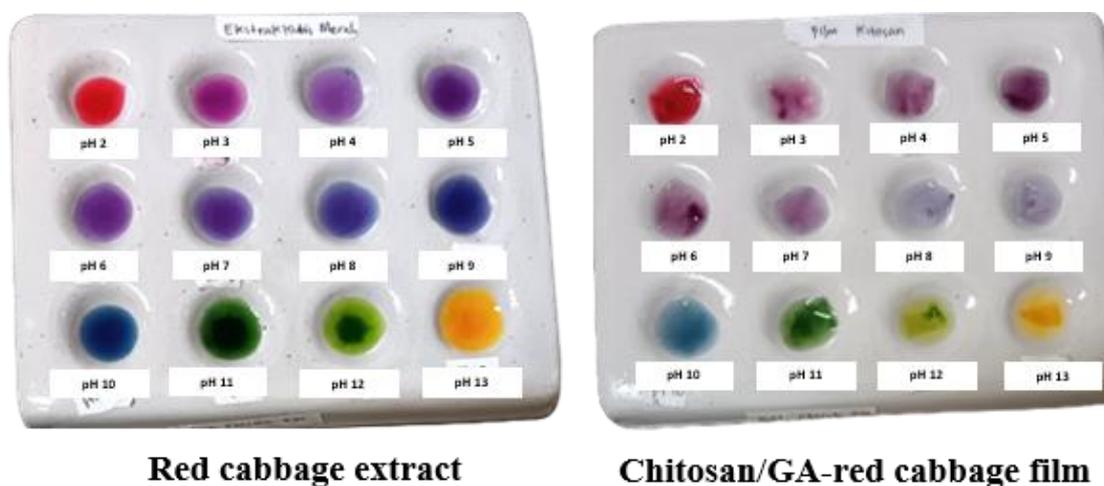

Figure 1 pH response of (a) red cabbage extract, (b) chitosan/GA-red cabbage extract.

The pH sensitivity of the red cabbage extract and the chitosan/GA red cabbage film was evaluated, focusing on their responses to different pH levels, particularly through visible color changes. The anthocyanin response in the red cabbage extract and chitosan/GA-red cabbage film across various pH values (pH 2 - 13) is shown in **Figure 1**. A sensitive pH ranges from 2 to 13 was observed, with the color shifting from red to yellow. At pH 3, the extract appeared pink, transitioning to purple at pH 4. Between pH 5 - 7, the color darkened to a deep purple, then shifted to bluish-purple at pH 8 - 9. At pH 10 - 13, the color transitioned from blue to green and finally to yellow at pH 13. These results are consistent with previous research Cheng *et al.* [24], which demonstrated that red cabbage extract can function effectively as a natural acid-base indicator. The color changes are caused by structural changes in anthocyanins caused by pH. As pH levels rise, the structure changes from red flavynium cations to purple, green, and yellow. Beyond pH 7, stability decreases due to the formation of chalcone [25,26]. The color response of the pH-sensitive film mirrored the color transitions observed in the red cabbage extract.

Characterization and testing of chitosan/GA-red cabbage film

Fourier transforms infrared spectra (FTIR)

The FTIR spectra of the chitosan-red cabbage films with varying volumes of glutaraldehyde (GA) as a crosslinking agent are presented in **Figure 2**. A broad peak around 3296 cm⁻¹ corresponds to the O–H and N–H stretching vibrations, characteristic of hydroxyl and amine groups in chitosan. The intensity of this band decreases and slightly shifts with increasing GA concentration, indicating the formation of hydrogen bonds between GA and the functional groups of chitosan [27,28]. The peak at 2919 cm⁻¹ is attributed to C–H stretching vibrations, while the band at 1587 cm⁻¹ corresponds to N–H bending of primary amines. These peaks also show variations in intensity with increasing GA content, further suggesting molecular interactions. However, no distinct absorption band is observed near 1640 – 1660 cm⁻¹, which would typically indicate the formation of imine (C=N) linkages via Schiff base reactions. This absence suggests that the interaction between chitosan and glutaraldehyde in this study is predominantly non-covalent, occurring mainly through hydrogen bonding and physical interactions, rather than covalent crosslinking.

These results indicate that glutaraldehyde modified the film structure through secondary interactions that enhanced the compactness and molecular arrangement of the chitosan matrix, contributing to the improved mechanical and functional properties observed. The proposed interaction mechanism is illustrated in **Figure 3**, the interaction between glutaraldehyde (GA) and the chitosan matrix appears to occur primarily through physical interactions, notably hydrogen bonding [29]. These interactions are likely formed between the oxygen atoms of the aldehyde groups in GA and the hydrogen atoms of the hydroxyl or amino groups in chitosan. In addition, hydrogen bonding may also occur between chitosan molecules themselves. Previous studies [30-32] have reported the formation of covalent imine bonds (C=N) between the aldehyde groups of GA and the amine groups of chitosan, suggesting chemical cross-linking. However, in this study, no significant peak shifts were observed in the FTIR spectra across different GA concentrations. This indicates that hydrogen bonding predominates over covalent bonding, which may be attributed to the relatively low concentration of GA used in the formulations. Therefore, the interaction mechanism observed in this study may differ from previous reports due to the milder cross-linking conditions applied.

Tensile properties

The anticipated outcome of the interaction between chitosan and GA is that increasing the concentration of the cross-linking agent will enhance the tensile strength of the film, attributed to the formation of stronger intermolecular interactions between the polymer chains. As shown in **Figure 4**, the stress and strain measurements reflect the tensile strength and elongation properties of the film. Pure chitosan film exhibits the lowest tensile strength at 5 MPa. However, the addition of GA as a cross-linking agent significantly increases the tensile strength to approximately 15.8 MPa, marking a threefold improvement compared to the pure chitosan film.
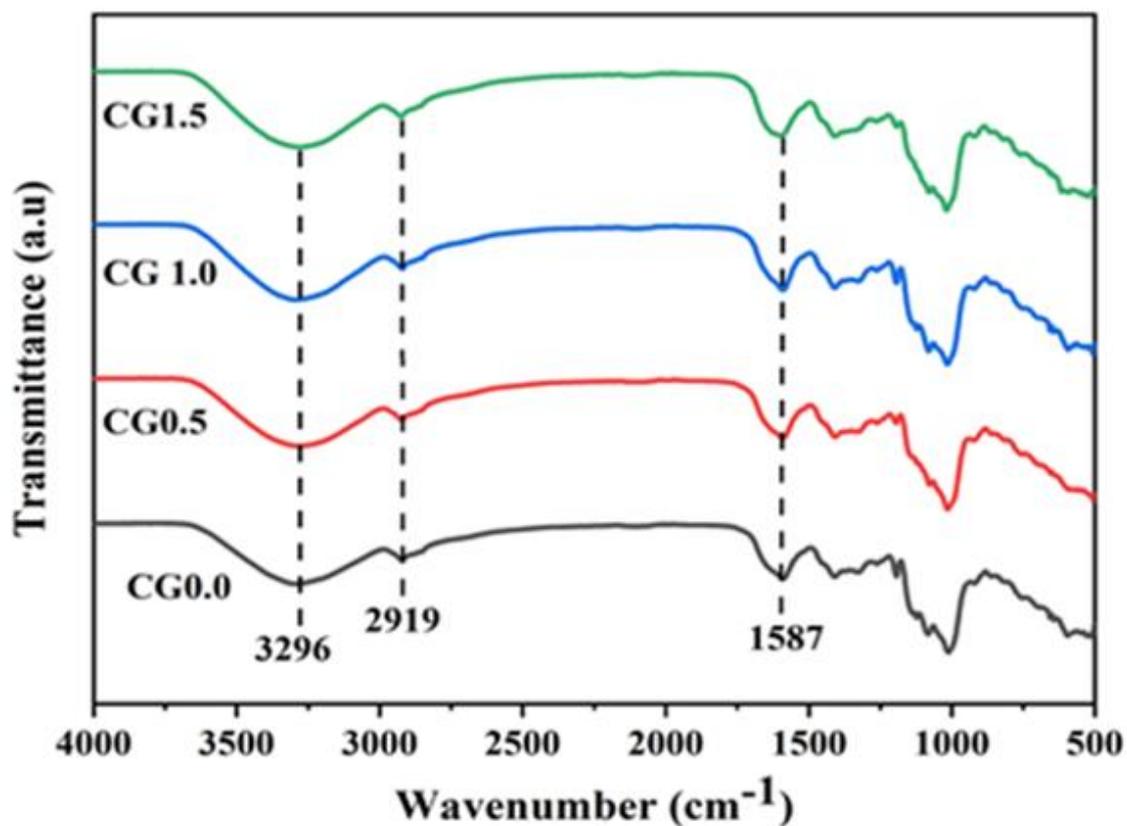
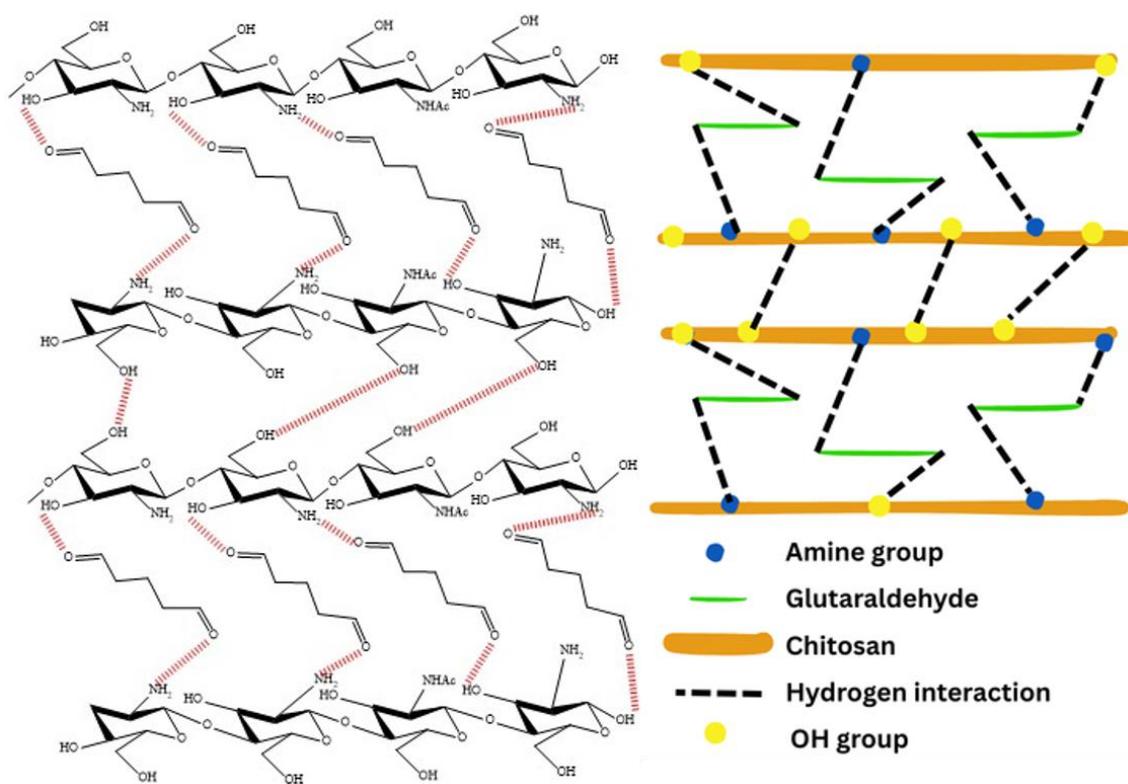**Figure 2** Fourier-transform IR spectra of chitosan/GA-red cabbage films.

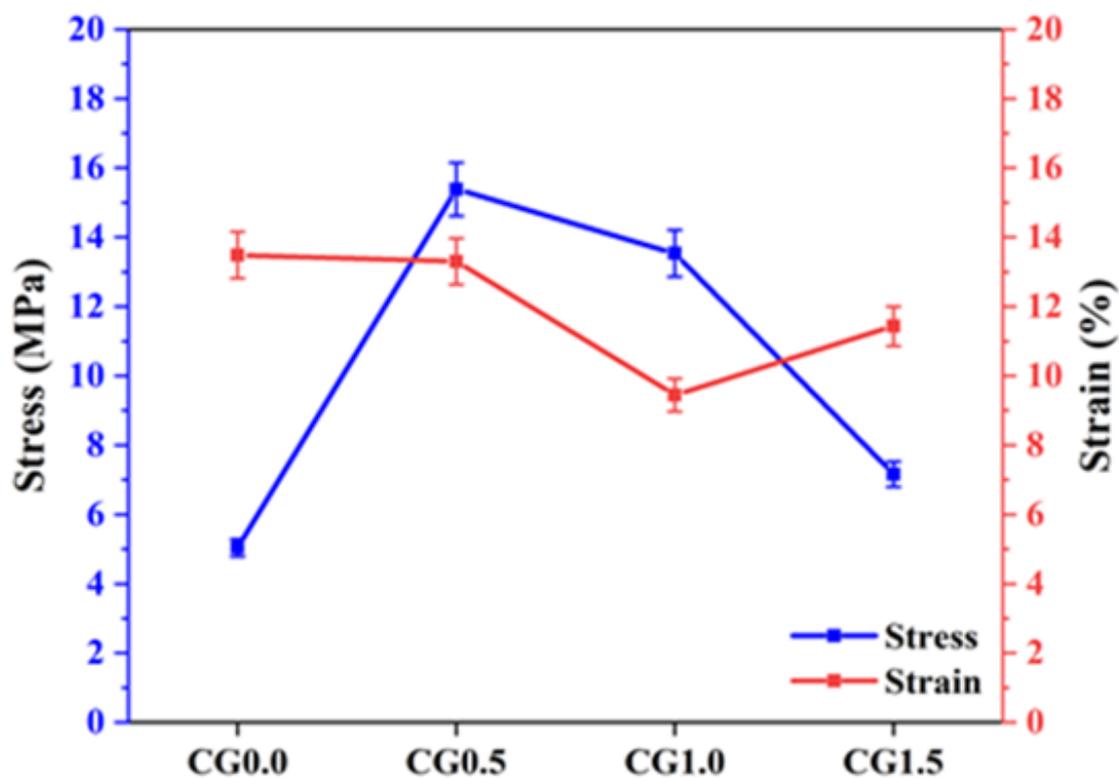**Figure 3** Proposed chitosan and glutaraldehyde interactions.

Figure 4 Stress and strain of chitosan/GA-red cabbage films.

Nevertheless, further addition of GA in the CG1.0 film reduces the tensile strength as the film becomes more brittle. Despite this reduction, the tensile strength still exceeds that of the pure chitosan film at 13.5 MPa, which is 2.5 times higher than that of the pure chitosan film. When the GA content is further increased in the CG1.5 film, the tensile strength drops to approximately 7.1 MPa, which remains 1.5 times higher than pure chitosan. The optimal tensile strength is achieved with 0.5 mL of GA, meeting the biodegradable plastic standards of 10 - 100 MPa [33].

The tensile strength of chitosan films cross-linked with glutaraldehyde shows a reverse trend as the GA volume increases at the same concentration. This trend is consistent with other studies Arianita *et al.* [34], Wegrzynowska *et al.* [35], which reported that a higher degree of GA cross-linking in chitosan films leads to reduced tensile strength. Although increasing GA may initially enhance cross-linking, an excessive amount can disrupt the uniformity of the polymer network, leading to phase separation, chain stiffness, or incomplete interactions. Furthermore, the presence of unreacted amine ($-NH_2$) or aldehyde groups may create internal stress or repulsive forces, which weaken the overall gel matrix [34].

The elongation percentage (strain) of pure chitosan shows the highest value, approximately 13%. The CG0.5 sample has an elongation percentage similar to pure chitosan. However, as the volume of cross-linking agents increases, the films become more brittle, leading to a decrease in elongation percentage. Chitosan cross-linked with GA has certain limitations, as higher levels of GA cause the film to become more fragile [31]. This observation is consistent with the research reported by another study Pavoni *et al.* [36], which indicated that increasing the concentration of GA in chitosan films reduces both tensile strength and elongation. In contrast, pure chitosan film exhibits the highest elongation value compared to those cross-linked with GA. The addition of GA to chitosan forms hydrogen bonds between chitosan polymers. However, if the cross-linking reaction is not well controlled, the resulting film may become weaker and brittle. Moreover, excessive GA can cause over-cross-linking, which stiffens the film and leads to a decline in mechanical strength and stability [37,38].
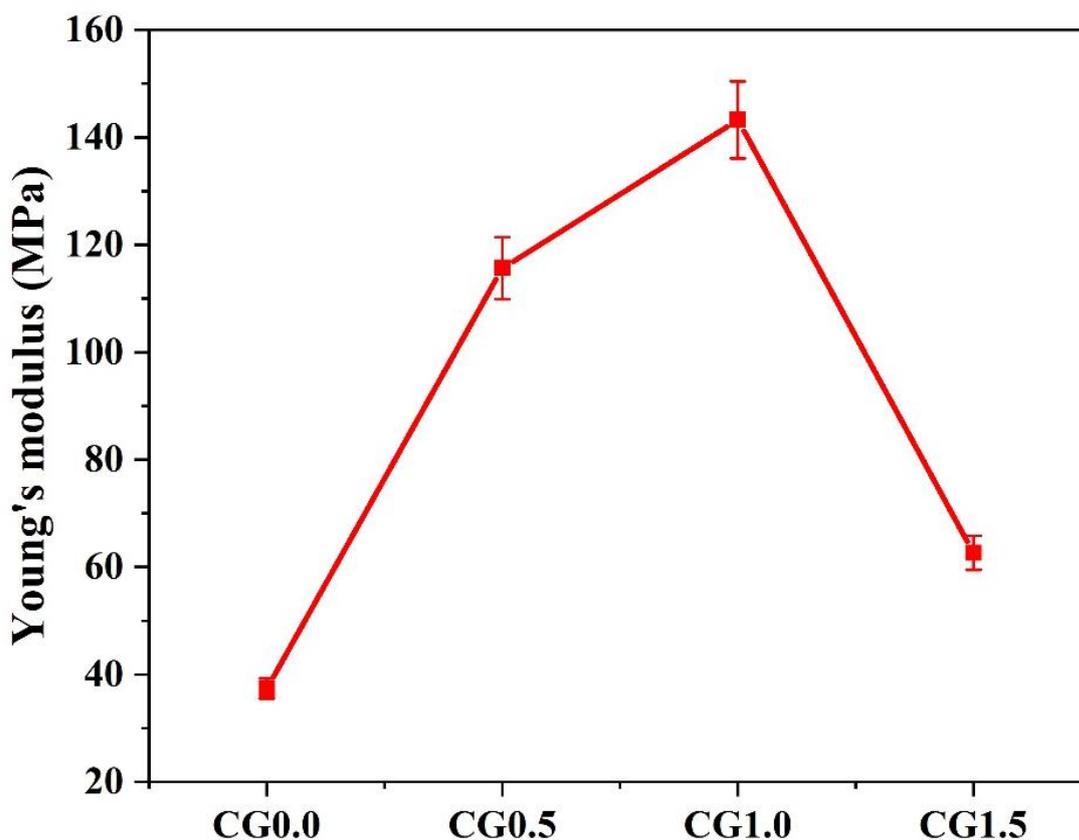
Figure 5 Young's modulus of the chitosan/GA-red cabbage films.

Young's modulus measures the elasticity of a material, providing insight into its hardness and resistance to elastic deformation under tensile or compressive stress. As shown in **Figure 5**, the Young's modulus of the pure chitosan is approximately 37 MPa, which is 3 - 3.8 times less than the chitosan films that include GA as a cross-linking agent. The increase in Young's modulus upon GA addition is attributed to the formation of hydrogen bonds between GA and the functional groups of chitosan, which strengthen the intermolecular interactions and reduce the mobility of polymer chains [39,40]. The CG1.0 film exhibits the highest modulus, indicating a more rigid structure. However, in the CG1.5 film, the Young's modulus decreases significantly. This may be due to excessive GA disrupting the uniformity of hydrogen bonding interactions, leading to a less organized and mechanically weaker matrix. Since no covalent cross-linking occurred in this system, the mechanical reinforcement depends solely on hydrogen bonding, which can become less effective when GA concentration is too high or unevenly distributed.

Field emission-scanning electron microscope (FE-SEM)

The surface and cross-sectional morphology of the films were analyzed using FE-SEM to assess both vertical and horizontal surface characteristics. As shown in **Figure 6 (a)** - **6(b)**, the surface of pure chitosan film appears relatively smooth, non-porous, and exhibits a plain texture, while the cross-sections display an irregular fibrous structure. Furthermore, the cross-section image of pure chitosan film (**Figure 6(b)**) clearly displays the microcracks in the films. **Figure 6(c)** - **6(d)** reveals that the surface of the chitosan/GA films is uneven, likely due to the impact of GA. The surface of the chitosan/GA film exhibits a nicely ordered network structure, which confirms that the crosslinking structure between chitosan and GA has been successfully formed. The cross-section shows a denser, orderly fibrous structure, indicating the effect of cross-linking by glutaraldehyde. These findings are in agreement with a study reported by [41].

The cross-sectional morphology directly influences the mechanical properties of the chitosan/GA

films (**Figure 6(b)** and **6(d)**). Adding a cross-linking agent results in a denser film structure, leading to higher tensile strength than pure chitosan film. This finding aligns with research conducted by Valizadeh *et al.* [42], Jufri *et al.* [43], which demonstrated that chitosan films cross-linked with GA exhibit greater tensile strength than pure chitosan film. Furthermore, the calculated porosity percentages are approximately 10% for pure chitosan and 7% for chitosan-GA, indicating that the

GA cross-linking reduces the film's porosity, resulting in a denser structure and consequently enhancing the tensile strength (stress) of chitosan/GA films. This observation is further supported by the study by Carolis *et al.* [44], which explains that the pore distribution within a material significantly influences its elasticity modulus, including stress, strain, and Young's modulus. The study concluded that as pore distribution increases, the modulus value decreases.
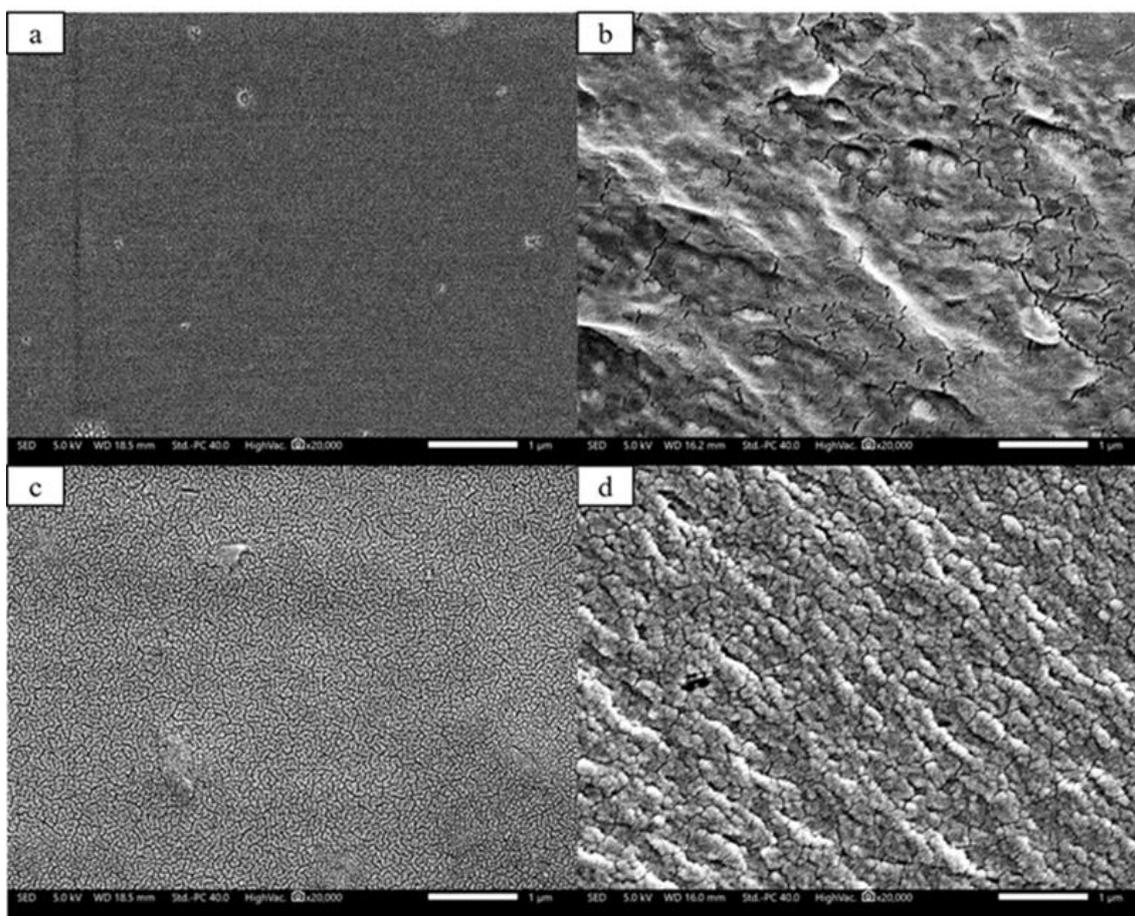

Figure 6 FE-SEM morphology: a. CG0.0 surface; b. CG0.0 cross-section; c. CG0.5 surface; d. CG0.5 cross section.

Contact angle

Contact angle measurement is employed to evaluate the hydrophilic or hydrophobic characteristics of a material. As shown in **Figure 7**, a lower contact angle indicates greater hydrophilicity of the film. The study reveals that the films exhibit contact angles ranging from 48.5° to 68.4°. The pure chitosan film (CG0.0) has a contact angle of 56.0°, which initially increases with addition of glutaraldehyde, reaching the highest value in the CG0.5 film (68.4°). This increase indicates a more hydrophobic surface, which can be

attributed to the formation of a denser and more compact structure due to the crosslinking between glutaraldehyde and chitosan. The GA molecules interact with hydroxyl ($-OH$) and amine ($-NH_2$) groups of chitosan mainly through hydrogen bonding, forming a tigher polymer network that reduces the availability of hydrophilic functional groups on the surface [45]. As a result, fewer water molecules can interact with the film surface, leading to a higher contact angle.

Interestingly, the contact angle decreases in CG1.0 and CG1.5 films, showing values lower than that of the

pure chitosan film. This unexpected trend may be explained by the excessive amount of GA distruping the optimal network structure. At higher GA concentration, over-crosslinking may occur, leading to a less uniform and more irregular surface morphology [46]. Moreover, the presence of unreacted aldehyde groups in the film matrix, which are polar, may increase the surface affinity for water. This results in an increase in hydrophilicity and a corresponding decrease in contact angle. Although the initial crosslinking improves hydrophobicity, excessive GA introduces polar sites and possible surface defects, reversing this effect [19].

This explanation is further supported by FE-SEM analysis (**Figure 6**), where the surface of the pure chitosan film (CG0.0) appears relatively smooth and homogeneous, whereas the CG0.5 film displays a denser and more compact morphology. These morphological differences support the observed trend in contact angles, suggesting that both chemical interactions and physical surface structure contribute to the wettability behavior of the films [47].
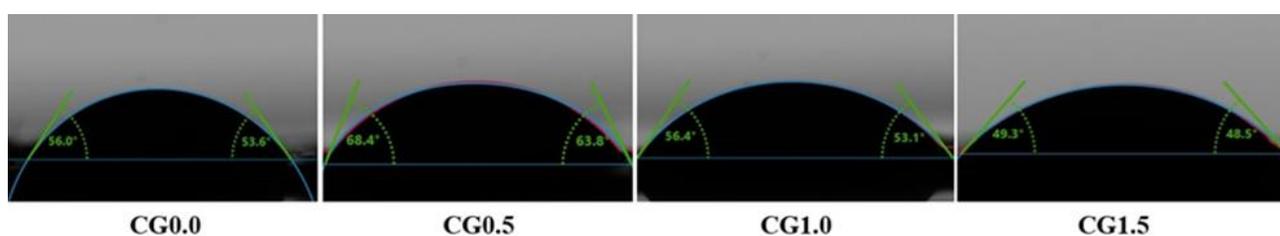

Figure 7 Schematic diagram of water contact.

Antibacterial activity

The antibacterial activity of the chitosan films incorporating GA is illustrated in **Figure 8**. The addition of GA into the chitosan films endows the films with antibacterial properties, as evidenced by the formation of inhibition zones against the gram-positive bacteria *S. aureus*. **Figure 8(a)**. shows that pure chitosan exhibits no inhibition zone, indicating a lack of antibacterial activity. In contrast, the CG0.5, CG1.0, and CG1.5 films demonstrate inhibition zones of 4.9 mm, 2.9 mm, and 3.9 mm, respectively. **Figure 8(b)**. displays the clear zones surrounding the samples.

Interestingly, although all GA-containing films demonstrate antibacterial activity, the CG0.5 film exhibits the largest inhibition zone. This suggests that the optimal antibacterial effect occurs at this concentration. The enhancement in antibacerial activity can be attributed to the interaction between the active $-NH_3^+$ groups of chitosan and the negatively charged components of bacterial cell walls, which disrupts cell membrane integrity and inhibits bacterial growth. The incorporation of GA id known to improve the structural stability of chitosan films, potentially enhancing their biofunctional performance.

However, films with higher GA concentrations (CG1.0 and CG1.5) showed smaller inhibition zones compared to CG0.5. This reduction may be attributed to increased hydrogen bonding interactions between chitosan and GA at higher concentrations. Excessive hydrogen bonding can lead to a denser polymer network, limiting the availability and diffusion of active $-NH_3^+$ groups responsible for antibacterial action. Consequently, this structural compactness may reduce the films' ability to interact with bacterial cells, leading to lower antibacterial effectiveness [48].

This observation on consistent with previous studies Li *et al.* [19], which reported that chitosan/GA films exhibited improved antibacterial performance compared to pure chitosan. However, an excessive amount of GA may lead to over-crosslinking, reducing the accessibility of active groups and ultimately affecting antibacterial efficacy.

Film soil degradability

The purpose of burying the film in soil is to evaluate its biodegradability by measuring weight loss over time. The gradual reduction in film mass indicates successful degradation. Chitosan films cross-linked with varying concentrations of GA are tested for their biodegradability over 5 days. As shown in **Figure 9**, the weight loss varied significantly, depending on the GA concentration. The pure chitosan film (CG0.0) exhibits

the fastest degradation rate, with a weight loss of approximately 65% after 5 days. The CG1.0 and CG1.5 films also showed relatively high degradation, with weight losses of around 58 and 55%, respectively. In contrast, the CG0.5 film demonstrated the lowest degradation rate, with a weight loss of about 50%. These findings indicate that while pure chitosan degrades rapidly, the addition of GA alters the film structure and reduces biodegadability, although the effect does not increase linearly with GA concentration. This result

aligns with Vikhoreva *et al.* [49], who reported that pure chitosan films fully decomposed within 5 - 7 days. In addition, Oberlintner *et al.* [50] reported that chitosan can degrade in soil with approximately 80% mass loss within 7 days of burial, demonstrating its rapid biodegradability under natural conditions. It is important to acknowledge that soil pH and moisture content, which were not measured in this study, could potentially influence the observed biodegradation behavior, as reported by previous studies [51].
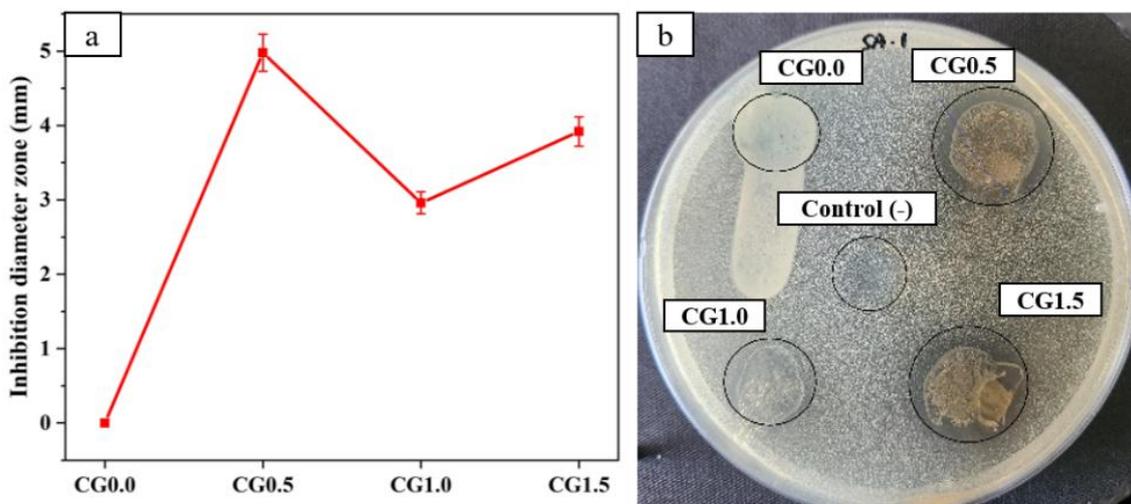

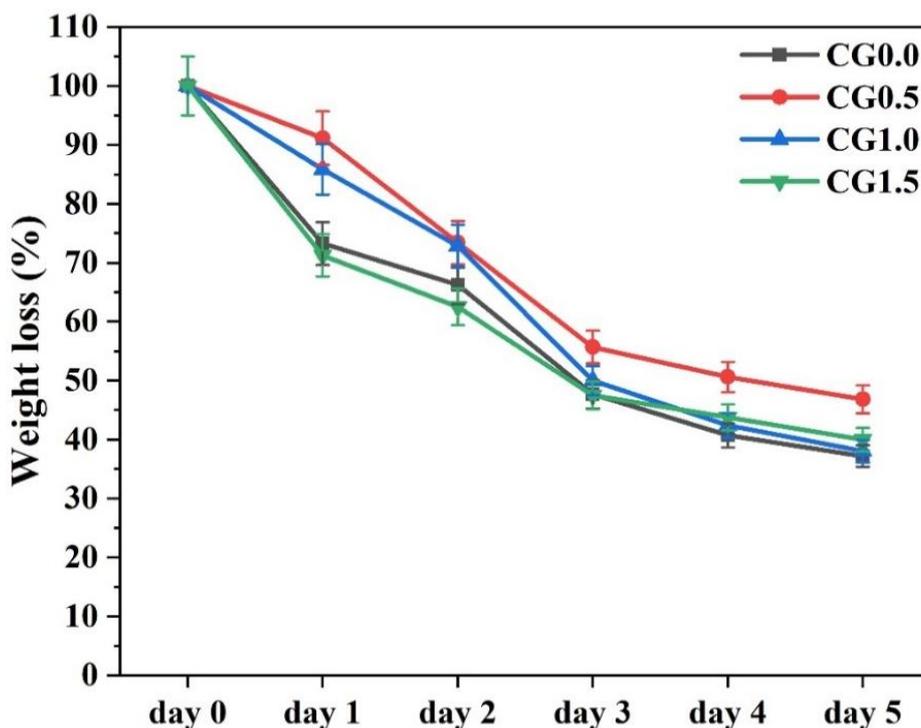**Figure 8** a. Antibacterial inhibition zone; b. clear zone of CG-red cabbage films (24 h).

Figure 9 Biodegradable test of CG-red cabbage films.

Film transparency

The appearance and color of food packaging sensors are essential in determining meat freshness labels and attracting consumer interest. As illustrated in **Figure 10**, the chitosan/GA film exhibits a clear color appearance with high transparency. This appearance is attributed to its composition of only chitosan and GA polymers, which are inherently transparent and lack additional particles or pigments. Consequently, it allows light to pass through the film. However, when coated with red cabbage extract, the film turns purple, leading to a reduction in transparency. This change is due to the presence of anthocyanin pigments, which absorb some of the light passing through the film. The transparency and light transmission decrease after the incorporation of chromophores and natural particles [52,53]. Similarly, recent studies have shown that the addition of alizarin to chitosan films significantly reduces transparency due to the deep red pigments of dihydroxyanthraquinone found in alizarin [54].

Figure 10 Visual transparency of (a) CG0.5 film; (b) CG0.5-red cabbage film.

Application of chitosan/GA-red cabbage film for monitoring of chicken freshness

Chitosan/GA-red cabbage films are applied to monitor chicken meat spoilage during storage at room temperature. The films demonstrate a clear response to spoilage by undergoing distinct color changes. At the start of storage (0 h), the film appears dark purple, reflecting the stability of anthocyanins under acidic conditions [8,10]. Fresh meat typically has a pH of 5.5 - 6.0. After 24 h of storage, the pH of the meat begins to rise due to spoilage microorganisms producing basic compounds such as ammonia and trimethylamine [55,56]. This increase in pH causes chemical structural changes in the anthocyanins, resulting in the film's color shifting to dark bluish-green. The spoilage-induced color change is shown in **Figure 11**. The pure chitosan film (CG0.0) exhibits faster and more pronounced color change compared to the chitosan films with GA (CG0.5, CG1.0, and CG1.5). This finding suggests that the addition of GA to the film enhances the stability of anthocyanins against pH changes during meat storage. Visual color changes in the film effectively indicate the freshness and spoilage of food [57]. In this study, fresh chicken meat has an initial pH of approximately 5.77, which increases to around 7 after 24 h of spoilage and reaches 8 by the end of the storage period, turning the film green (**Table 2**). These findings align with observations by Chaithra *et al.* [58], Fang *et al.* [59], who reported similar color transitions from purple to green during prolonged storage. Kanatt *et al.* [25] reported that fresh chicken generally has a pH of approximately 5.5 as spoilage progresses, the pH rises beyond 6, primarily due to microbial activity and the action of endogeneous proteolytic enzymes. These enzymes catalyze the breakdown of proteins, producing basic compounds such as ammonia and amines, which contribute to the increase in pH.
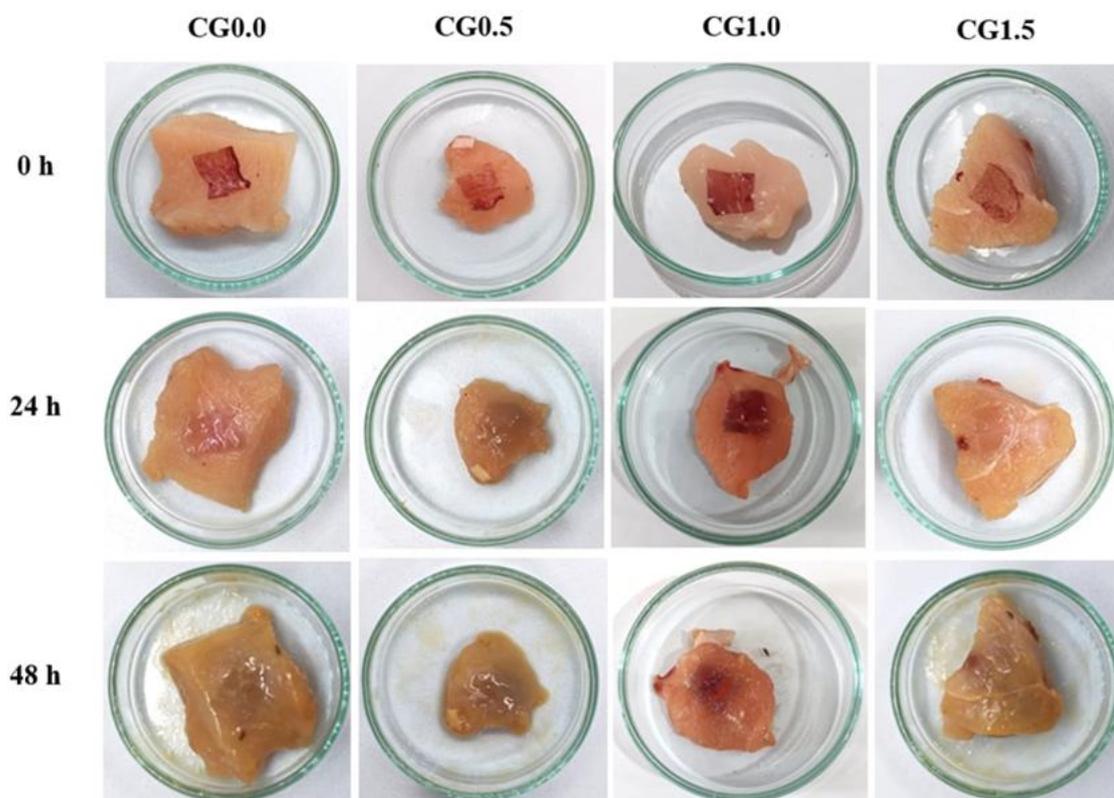
Figure 11 Color changes of chitosan/GA-red cabbage films during chicken meat storage.

Table 2 Color changes of sensor film based on storage time and meat pH.

Time (h)	Film color	pH	Meat condition
0	Purple	5.77	Fresh
24	Dark blush green	7.0	Less fresh
48	green	8.0	Spoilage

Conclusions

The chitosan-GA films coated with red cabbage extract were successfully developed as biodegradable, colorimetric indicators for monitoring meat freshness. Among the tested formulations, the film containing 0.5% GA (CG0.5) demonstrated a favorable combination of properties, including enhanced antibacterial activity, improved tensile strength, and a distinct pH-responsive color transition. The addition of red cabbage extract effectively enabled the film to visually indicate meat spoilage. In terms of biodegradability, the pure chitosan film degraded by approximately 60% within 5 days, whereas the GA-crosslinked films showed slower degradation rates, influenced by the GA concentration. Overall, these results suggest that the developed chitosan-based film has strong potential as a sustainable freshness indicator, with adjustable degradation behavior tailored through crosslinker content.

Declaration of Generative AI in Scientific Writing

The authors declare that generative AI tools (e.g., ChatGPT by OpenAI) were used during the preparation of this manuscript to assist with improving the clarity of language and grammar. No AI tool was used to generate original scientific content, data, or to draw scientific conclusions. All data analysis, interpretation, and critical revisions were conducted solely by the authors.

CRediT Author Statement

Faza Ilya Sururim Masfufah: Investigation, Methodology, Writing - Original Draft.

Ngadiwiyana Ngadiwiyana: Supervision.

Yassaroh Yassaroh: Writing - Review & Editing.

Retno Wulandari: Formal analysis.

Nor Basid Adiwibawa Prasetya: Conceptualization, Writing - Original Draft, Writing - Review & Editing, Supervision.

References

[1] M Alizadeh-Sani, E Mohammadian, J-W Rhim and SM Jafari. pH-sensitive (halochromic) smart packaging films based on natural food colorants for the monitoring of food quality and safety. *Trends in Food Science & Technology* 2020; **105**, 93-144.

[2] A Bahrami, R Delshadi, E Assadpour, SM Jafari and L Wiliams. Antimicrobial-loaded nanocarriers for food packaging applications. *Advances in Colloid and Interface Science* 2020; **278**, 102140.

[3] J Liu, F Xie, R Li and T Li. TiO_2-x/Ag_3PO_4 photocatalyst: Oxygen vacancy dependent visible light photocatalytic performance and BPA degradative pathway. *Materials Science in Semiconductor Processing* 2019; **97**, 1-10.

[4] T Vo, T Dang and B Chen. Synthesis of intelligent pH indicative films from chitosan/poly (vinyl alcohol)/anthocyanin extracted from red cabbage. *Polymers* 2019; **11(7)**, 1088.

[5] M Chen, T Yan, J Huang and Y Zhou. Fabrication of halochromic smart films by immobilizing red cabbage anthocyanins into chitosan/oxidized-chitin nanocrystals composites for real-time hairtail and shrimp freshness monitoring.

International Journal of Biological Macromolecules 2021; **179**, 90-100.

[6] X Li, J S del Río Saez, S Du, RS Diaz, X Ao and D Wang. Bio-based chitosan-based film as a bifunctional fire-warning and humidity sensor. *International Journal of Biological Macromolecules* 2023; **253(3)**, 126466.

[7] Y Liu, G Chen, Y Yang, R Wu, L Zhang, W Mu and S Wang. Fabrication of chitosan-based smart film by the O/W emulsion containing curcumin for monitoring pork freshness. *Journal of Food Engineering* 2024; **379**, 112115.

[8] L Prietto, TC Mirapalhete, VZ Pinto, JF Hoffmann, NL Vanier, L Lim, ARG Dias and EDR Zavareze. pH-sensitive films containing anthocyanins extracted from black bean seed coat and red cabbage. *Lwt* 2017; **80**, 492-500.

[9] M Shahid, Shahid-ul-Islam, F Mohammad. Recent advancements in natural dye applications: A review. *Journal of Cleaner Production* 2013; **53**, 310-331.

[10] S Roy and J Rhim. Anthocyanin food colorant and its application in pH-responsive color change indicator films. *Critical Reviews in Food Science and Nutrition* 2021; **61(14)**, 2297-2325.

[11] L Cao, G Sun, C Zhang, W Liu, J Li and L Wang. An intelligent film based on cassia gum containing bromothymol blue-anchored cellulose fibers for real-time detection of meat freshness. *Journal of Agricultural and Food Chemistry* 2019; **67(7)**, 2066-2074.

[12] L Ding, X Li, L Hu, Y Zhang, Y Jiang, Z Mao, H Xu, B Wang, X Feng and X Sui. A naked-eye detection polyvinyl alcohol/cellulose-based pH sensor for intelligent packaging. *Carbohydrate Polymers* 2020; **233**, 115859.

[13] Y Zhao, J Du, H Zhou, S Zhou, Y Lv, Y Cheng, Y Tao, J Lu and H Wang. Biodegradable intelligent film for food preservation and real-time visual detection of food freshness. *Food Hydrocolloids* 2022; **129**, 107665.

[14] YS Musso, PR Salgado and AN Mauri. Smart gelatin films prepared using red cabbage (*Brassica oleracea L.*) extracts as solvent. *Food Hydrocolloids* 2019; **89**, 674-681.

[15] T Gasti, S Dixit, OJ D'souza, VD Hiremani, SK Vootla, SP Masti, RB Chougale and RB Malabadi.

Smart biodegradable films based on chitosan/methylcellulose containing Phyllanthus reticulatus anthocyanin for monitoring the freshness of fish fillet. *International Journal of Biological Macromolecules* 2021; **187**, 451-461.

[16] J Liang and R Chen. Impact of cross-linking mode on the physical properties of zein/PVA composite films. *Food Packaging and Shelf Life* 2018; **18**, 101-106.

[17] H Deng, W Zhang, Y Ramezan, Z Riahi, A Khan and Z Huang. Antibacterial and antioxidant plant-derived aldehydes: A new role as cross-linking agents in biopolymer-based food packaging films. *Comprehensive Reviews in Food Science and Food Safety* 2025; **24(1)**, e70089.

[18] T Hasanvand, M Mohammadi, F Abdollahpour, B Kamarehie, A Jafari, A Ghaderpoori and MA Karami. A comparative study on antibacterial activity of carvacrol and glutaraldehyde on Pseudomonas aeruginosa and *Staphylococcus aureus* isolates: An *in vitro* study. *Journal of Environmental Health Science and Engineering* 2021; **19**, 475-482.

[19] B Li, C Shan, Q Zhou, Y Fang, Y Wang, F Xu, L Han, M Ibrahim, L Guo, G Xie and G Sun. Synthesis, characterization, and antibacterial activity of cross-linked chitosan-glutaraldehyde. *Marine Drugs* 2013; **11(5)**, 1534-1552.

[20] ACD Araujo, JP Gomes, FBD Silva, JS Nunes, FSD Santos, WPD Silva, JPDL Ferreira, AJDM Queiroz, RMFD Figueiredo, GSD Lima, LADA Soares, APT Rocha and AGBD Lima. Optimization of extraction method of anthocyanins from red cabbage. *Molecules* 2023; **28(8)**, 3549.

[21] AB Das, VV Goud and C Das. Extraction of phenolic compounds and anthocyanin from black and purple rice bran (Oryza sativa L.) using ultrasound: A comparative analysis and phytochemical profiling. *Industrial Crops and Products* 2017; **95**, 332-341.

[22] LMD Oliveira, and F Antelo. Thermostability of the visual color and anthocyanins from Rio-Grande-Cherry (Eugenia involucrata DC). *Brazilian Journal of Food Technology* 2020; **23**, e2019140.

[23] HE Khoo, A Azlan, ST Tang and SM Lim. Anthocyanidins and anthocyanins: Colored pigments as food, pharmaceutical ingredients, and the potential health benefits. *Food & Nutrition Research* 2017; **61**, 1361779.

[24] M Cheng, X Yan, Y Cui, M Han, X Wang, J Wang and R Zhang. An eco-friendly film of pH-responsive indicators for smart packaging. *Journal of Food Engineering* 2022; **321**, 110943.

[25] SR Kanatt. Development of active/intelligent food packaging film containing Amaranthus leaf extract for shelf life extension of chicken/fish during chilled storage. *Food Packaging and Shelf Life* 2020; **24**, 100506.

[26] T Liang, G Sun, L Cao, J Li and W Wang. A pH and NH_3 sensing intelligent film based on Artemisia sphaerocephala Krasch. gum and red cabbage anthocyanins anchored by carboxymethyl cellulose sodium added as a host complex. *Food Hydrocolloids* 2019; **87**, 858-868.

[27] Y Liu, Z Cai, L Sheng, M Ma, Q Xu and Y Jin. Structure-property of crosslinked chitosan/silica composite films modified by genipin and glutaraldehyde under alkaline conditions. *Carbohydrate Polymers* 2019; **215**, 348-357.

[28] F Doustdar, A Olad and M Ghorbani. Effect of glutaraldehyde and calcium chloride as different crosslinking agents on the characteristics of chitosan/cellulose nanocrystals scaffold. *International Journal of Biological Macromolecules* 2022; **208**, 912-924.

[29] EC Stroparo, KC Mollinari and KVD Souza. Use of chitosan in the remediation of water from purification of biodiesel. *Polimeros* 2018; **28(5)**, 400-405.

[30] FF Illiana and HD Ariyanto. Development of chitosan/glutaraldehyde cross-linked film with silica addition as membrane material for SLS rejection in detergent wastewater. *Journal of Vocational Studies on Applied Research* 2024; **6(1)**, 1-6.

[31] JM Frick, A Ambrosi, LD Pollo and IC Tessaro. Influence of glutaraldehyde crosslinking and alkaline post-treatment on the properties of chitosan-based films. *Journal of Polymers and the Environment* 2018; **26**, 2748-2757.

[32] NR Kildeeva, PA Perminov, LV Vladimirov, VV Novikov and SN Mikhailov. About mechanism of chitosan cross-linking with glutaraldehyde. *Russian Journal of Bioorganic Chemistry* 2009; **35**, 360-369.

[33] HD Rahmayanti, A Zulfi, JC Ginting, TR Kartika, S Ardiani, N Akmalia and M Dioktyanto. Physicomechanical properties of edible film-based nata de coco, acetic acid, and Chitosan. *KnE Engineering* 2024; **2024**, 668-674.

[34] A Arianita, Cahyaningtyas, B Amalia, W Pudjiastuti, S Melanie, V Fauzia and C Imawan. Effect of glutaraldehyde to the mechanical properties of chitosan/nanocellulose. *Journal of Physics: Conference Series* 2019; **1317**, 012045.

[35] K Wegrzynowska-Drzymalska, P Grebicka, DT Mlynarczyk, D Chelminiak-Dudkiewicz, H Kaczmarek, T Goslinski and M Ziegler-Borowska. Crosslinking of chitosan with dialdehyde chitosan as a new approach for biomedical applications. *Materials* 2020; **13(15)**, 3413.

[36] JMF Pavoni, NZD Santos, IC May, LD Pollo and IC Tessaro. Impact of acid type and glutaraldehyde crosslinking in the physicochemical and mechanical properties and biodegradability of chitosan films. *Polymer Bulletin* 2021; **78**, 981-1000.

[37] J Galan, J Trilleras, PA Zapata, VA Arana and CD Grande-Tovar. Optimization of chitosan glutaraldehyde-crosslinked beads for reactive blue 4 anionic dye removal using a surface response methodology. *Life* 2021; **11(2)**, 85.

[38] RV Pinto, PS Gomes, MH Fernandes, MEV Costa and MM Almeida. Glutaraldehyde-crosslinking chitosan scaffolds reinforced with calcium phosphate spray-dried granules for bone tissue applications. *Materials Science and Engineering: C* 2020; **109**, 110557.

[39] REK Billah, M Ahrouch, L Bahsis, N Aflak, Z Azoubi, H Majdoubi, M Achak, Y Abdellaoui and MA Khan. Biological activity assessment and water deflouridation application of glutaraldehyde crosslinked chitosan-TiO2 composite: A conjugated experimental and theoretical insights. *Separation and Purification Technology* 2025; **368**, 132984.

[40] L Poon, LD Wilson, and JV Headley. Chitosan-glutaraldehyde copolymers and their sorption properties. *Carbohydrate Polymers* 2014; **109**, 92-101.

[41] W Sun, S Kothari and CC Sun. The relationship among tensile strength, Young's modulus, and indentation hardness of pharmaceutical compacts. *Powder Technology* 2018; **331**, 1-6.

[42] S Valizadeh, M Naseri, S Babaei, SMH Hosseini and A Imani. Development of bioactive composite films from chitosan and carboxymethyl cellulose using glutaraldehyde, cinnamon essential oil and oleic acid. *International Journal of Biological Macromolecules* 2019; **134**, 604-612.

[43] M Jufri, RA Lusiana and NBA Prasetya. Effects of additional polyvinyl alcohol (PVA) on the physiochemical properties of chitosan-glutaraldehyde-gelatine bioplastic. *Jurnal Kimia Sains dan Aplikasi* 2022; **25(3)**, 130-136.

[44] SD Carolis, C Putignano, L Soria and G Carbone. Effect of porosity and pore size distribution on elastic modulus of foams. *International Journal of Mechanical Sciences* 2024; **261**, 108661.

[45] Y Gao, K Peng and S Mitragotri. Covalently crosslinked hydrogels via step-growth reactions: Crosslinking chemistries, polymers, and clinical impact. *Advanced Materials* 2021; **33(25)**, 2006362.

[46] D Kim, INMD Chan, TMS Manalastas, RSC II, JRHS Agueda and RKB Bitangcor. Optimization of glutaraldehyde concentration in relation to swelling behavior of PVA-PEG-BTB film using hybrid genetic metaheuristic algorithm. *Scientific Reports* 2025; **15**, 12582.

[47] IS Bayer and CM Megaridis. Contact angle dynamics in droplets impacting on flat surfaces with different wetting characteristics. *Journal of Fluid Mechanics* 2006; **558**, 415-449.

[48] FS Jebel and H Almasi. Morphological, physical, antimicrobial and release properties of ZnO nanoparticles-loaded bacterial cellulose films. *Carbohydrate Polymers* 2016; **149**, 8-19.

[49] G Vikhoreva, N Kil'deeva, MY Ustinov, and YN Nochevkina. Fabrication and study of the degradability of chitosan films. *Fibre Chemistry* 2002; **34**, 407-411.

[50] A Oberlintner, M Bajic, G Kalcikova, B Likozar, B Likozar and U Novak. Biodegradability study of active chitosan biopolymer films enriched with Quercus polyphenol extract in different soil types. *Environmental Technology & Innovation* 2021; **21**, 101318.

[51] S Nizamuddin, AJ Baloch, C Chen, M Arif and NM Mubarak. Bio-based plastics, biodegradable plastics, and compostable plastics: Biodegradation mechanism, biodegradability standards and environmental stratagem. *International Biodeterioration & Biodegradation* 2024; **195**, 105887.

[52] M Alizadeh-Sani, M Tavassoli, DJ McClements and H Hamishehkar. Multifunctional halochromic packaging materials: Saffron petal anthocyanin loaded-chitosan nanofiber/methyl cellulose matrices. *Food Hydrocolloids* 2021; **111**, 106237.

[53] MA Sani, M Tavassoli, H Hamishehkar and DJ McClements. Carbohydrate-based films containing pH-sensitive red barberry anthocyanins: Application as biodegradable smart food packaging materials. *Carbohydrate Polymers* 2021; **255**, 117488.

[54] P Ezati and J Rhim. pH-responsive chitosan-based film incorporated with alizarin for intelligent packaging applications. *Food Hydrocolloids* 2020; **102**, 105629.

[55] M Nami, M Taheri, J Siddiqui, IA Deen, M Packirisamy and MJ Deen. Recent progress in intelligent packaging for seafood and meat quality monitoring. *Advanced Materials Technologies* 2024; **9(12)**, 2301347.

[56] D Komodromos, D Sergelidis, I Amvrosiadis and MG Kontominas. Combined effect of an active agIon® absorbent pad and a chitosan coating on the preservation of fresh beef. *Foods* 2024; **13(9)**, 1387.

[57] M Nadi, SMA Razavi and D Shahrampour. Fabrication of green colorimetric smart packaging based on basil seed gum/chitosan/red cabbage anthocyanin for real-time monitoring of fish freshness. *Food Science & Nutrition* 2023; **11(10)**, 6360-6375.

[58] KP Chaithra, TP Vinod and P Nagarajan. Smartphone application-based colorimetric fish freshness monitoring using an indicator prepared by rub-coating of red cabbage on paper substrates. *Colloids and Surfaces A: Physicochemical and Engineering Aspects* 2023; **679**, 132553.

[59] S Fang, Z Guan, C Su, W Zhang, J Zhu, Y Zheng, H Li, P Zhao and X Liu. Accurate fish-freshness prediction label based on red cabbage anthocyanins. *Food Control* 2022; **138**, 109018.